

**PRE-PROTOSTELLAR AND LOW-MASS STAR
FORMING CLOUDS IN CEPHEUS**

S. NIKOLIĆ^{1,2}

¹*Astronomical Observatory, Volgina 7, 11160 Belgrade - 74, Serbia and Montenegro*

²*Onsala space Observatory, S-43992 Onsala, Sweden*

E-mail silvana@aob.aob.bg.ac.yu

Abstract. We present here an excerpt from the PhD thesis "Molecular clouds in the Cepheus region".

1. INTRODUCTION

The area between the Cepheus and Cassiopeia molecular cloud complexes ($115^\circ \leq \ell \leq 125^\circ$, $106^\circ \leq b \leq 20^\circ$) is virtually free of CO emission, with the "hole" filled with excess soft X-ray radiation probably caused by a supernova explosion roughly 10^4 years ago at a distance of 300 pc (Grenier et al. 1989). A ridge of the major radio-continuum Loop III runs along the eastern boundary of the Cepheus cloud complex (Berkhuijsen 1971). Loop III has an estimated distance of 150 pc and the projected center is $l \approx 125^\circ$, $b \approx 15^\circ$. It is generally accepted that the origin of these loops are old supernova remnants with ages estimated to $\sim 10^6$ years. The existence of a third SN-candidate is indicated by a runaway star HD 203854 in the Cepheus Flare region (Kun et al. 2000). The measured space velocity suggests that this star might have been a companion of a supernova some $5 \times 10^5 - 10^6$ years ago just inside the "Grenier-bubble".

We have selected several pre-protostellar and star forming clouds in this area for optical, IR and radio spectral line observations and studies with the purpose to trace the SN-induced shock legacy in the region. Here we present the main results for L 1274 and L 1251 dark clouds.

2. L 1274

L 1274 ($l \approx 118.52^\circ$, $b \approx 8.54^\circ$) is a small dark cloud whose projected location is close to a peak of excess soft X-ray emission (Grenier et al. 1989). The cloud was detected in several CO surveys. Yonekura et al. (1997) estimated from their ^{13}CO survey of the IIInd Galactic quadrant a peak hydrogen column density of $1.4 \times 10^{21} \text{ cm}^{-2}$ and derived a mass of $31 M_\odot$ (assumed distance of 300 pc). The cloud is classified as a pre-protostellar.

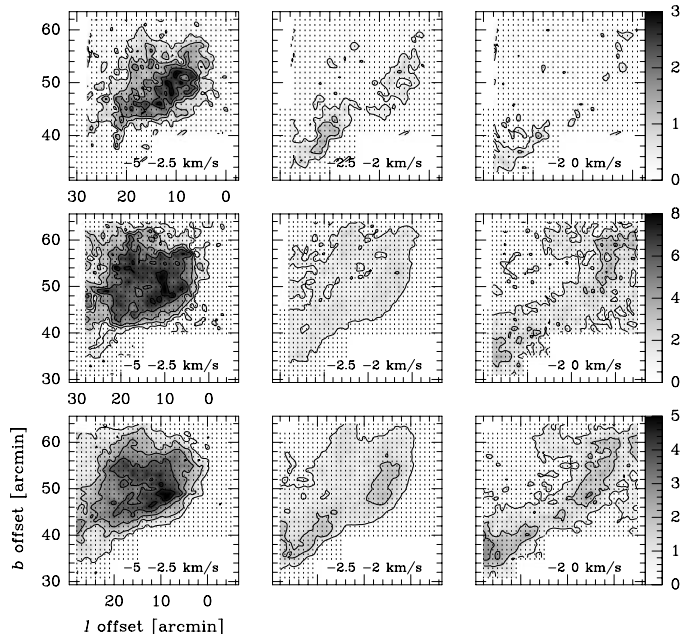


Figure 1: ^{13}CO (1–0) (first), ^{12}CO (1–0) (second) and ^{12}CO (2–1) (third row) channel maps. Covered velocity ranges are indicated in the lower right corner of each panel. The intensity scale is in $T_A^* dv$ [K km s^{-1}]. The observed positions are indicated by dots. Offsets are relative to $\ell = 118^\circ$, $b = 8^\circ$.

2. 1. DISTANCE AND DUST DISTRIBUTION

From our objective prism spectroscopy we derive a distance of 200 ± 30 pc to the cloud. The $100 \mu\text{m}$ excess emission, defined as $\Delta I_{100} = I_{100} - I_{60} / \Theta$, where Θ is the ratio I_{60}/I_{100} in the outer diffuse regions, for L 1274 is spatially very well correlated with the ^{13}CO emission, i.e., with molecular gas of densities $> 10^3 \text{ cm}^{-3}$.

2. 2. CO MAPS AND MASS ESTIMATES

Using the 20-m telescope of the Onsala Space Observatory and the 3-m KOSMA telescope we mapped the cloud in the $J = 1 - 0$ transition of ^{12}CO and ^{13}CO and in the $J = 2 - 1$ transition of ^{12}CO . Pointed measurements or cross-scans were made also in C^{18}O (1–0), CS (2–1), HCN (1–0), ^{12}CO (3–2), ^{13}CO (2–1), ^{13}CO (3–2) and C^{18}O (2–1). The CO channel maps in Fig. 1 show two distinct structures: the "main body" of the cloud emitting within the velocity range -5 to -2.5 km s^{-1} and the "ridge" which is seen between -2 and 0 km s^{-1} . At a distance of 200 pc the linear extent of the main body is 1.5 to 2 pc as defined by the lowest (10%) contours in the figure presented. In ^{13}CO (1–0) the main body is well defined while the ridge has barely any emission, indicating that the ridge consists of more diffuse gas. LTE and MEP analysis of the CO data resulted in an estimated $T_{kin} \approx T_{ex} = 10 \pm 2 \text{ K}$, $N(^{12}\text{CO}) = 4 \pm 1 \times 10^{17} \text{ cm}^{-2}$ and a H_2 -density of about $5 \times 10^3 \text{ cm}^{-3}$. However, the MEP solution for the detected HCN, assuming $T_{kin} = 10 \text{ K}$, gives a hydrogen density of $5 \times 10^4 \text{ cm}^{-3}$ and $N(\text{HCN}) = 10^{12} \text{ cm}^{-2}$.

Table 1: Estimates of distance and mass of the main body in L 1274. The errors are formal 1σ uncertainties. n_{H_2} is the mean density in a volume of radius r . ¹⁾ Diameter of the emission (50% contour). ²⁾ Radius of the emission (10% contour). ³⁾ Distance determined from the size–line width relation by Solomon et al. (1987).

		CO(1 – 0)	¹³ CO(1 – 0)	CO(2 – 1)
Δv	[km s ⁻¹]	1.51	1.12	1.65
d ¹⁾	[arcmin]	18.6	12.0	17.7
r ²⁾	[arcmin]	14	10	13
D ³⁾	[pc]	190	160	230
M_{vir}	[M _⊙]	370 ± 30	130 ± 8	420 ± 35
M_x	[M _⊙]	43 ± 4		
M_{13}	[M _⊙]		25 ± 2	
n_{H_2}	[cm ⁻³]	320	460	

In Table 1 we present mass estimates resulting from different methods. A crucial parameter is the distance and we have used 200 pc obtained from our optical measurements. The virial mass estimates are based on the relation $M_{vir} = 150 d \Delta v^2 [M_{\odot}]$ (Johansson et al. 1998). With a CO–to–H₂ conversion factor of $1.9 \times 10^{20} \text{ cm}^{-2} (\text{K km s}^{-1})^{-1}$ (Strong & Mattox 1996) and a correction for helium, the total gas mass estimated from the CO(1–0) data is $M_x = 4.13 L_{CO} [M_{\odot}]$, where L_{CO} is the CO–luminosity in units of $\text{K km s}^{-1} \text{ pc}^2$. A third estimate, M_{13} , from the ¹³CO emission, uses the ratio $[\text{H}_2]/[^{13}\text{CO}] = 4.8 \times 10^5$ (Dickman & Clemens 1983).

As seen in Table 1 derived virial masses are by a factor of 3–17 higher than other mass estimates. Yonekura et al. (1997) also find high M_{vir}/M_{13} ratios for clouds with $M_{13} \leq 100 M_{\odot}$. They estimate the external pressure in this region to $P_{ext}/k \sim 10^5 \text{ K cm}^{-3}$. This pressure is high enough to bind most of the clouds in their sample, except maybe the smallest ones. For L 1274, using the M_{13} mass estimate, we find that the pressure required to bind the main body is $\sim 10^{4.5} \text{ K cm}^{-3}$, an indication that the main body might be pressure confined.

In any case, L 1274 is apparently not gravitationally bound. This suggests that it is either formed by another process than gravitation or, disturbed by some internal or external process. Both cases might be explained by the passage of a shock front. In the former case, the shock front triggers the formation of a cloud, which, if gravitation does not take over, eventually evaporates. In the latter case, the shock front injects energy into the cloud, which may be seen, e.g., in the form of increased turbulence. No internal activity, core collapse or star formation, is detected, thus leaving the other option which alone could explain the difference between our mass estimates. Support for a passage of a shock front comes from the channel maps in Fig. 1 which indicate that the main body and the ridge component are related. In this scenario the ridge is an expanding low density feature that comes from the outer layers of the main body. Assuming that the ridge has been swept away in a collision with a SN–induced shock front, the relative motions of the main body and the ridge in the radial direction where the ridge has gained some positive peculiar velocity relative to the main body, are consistent with passage of a *slow* shock during the last 10^6 years.

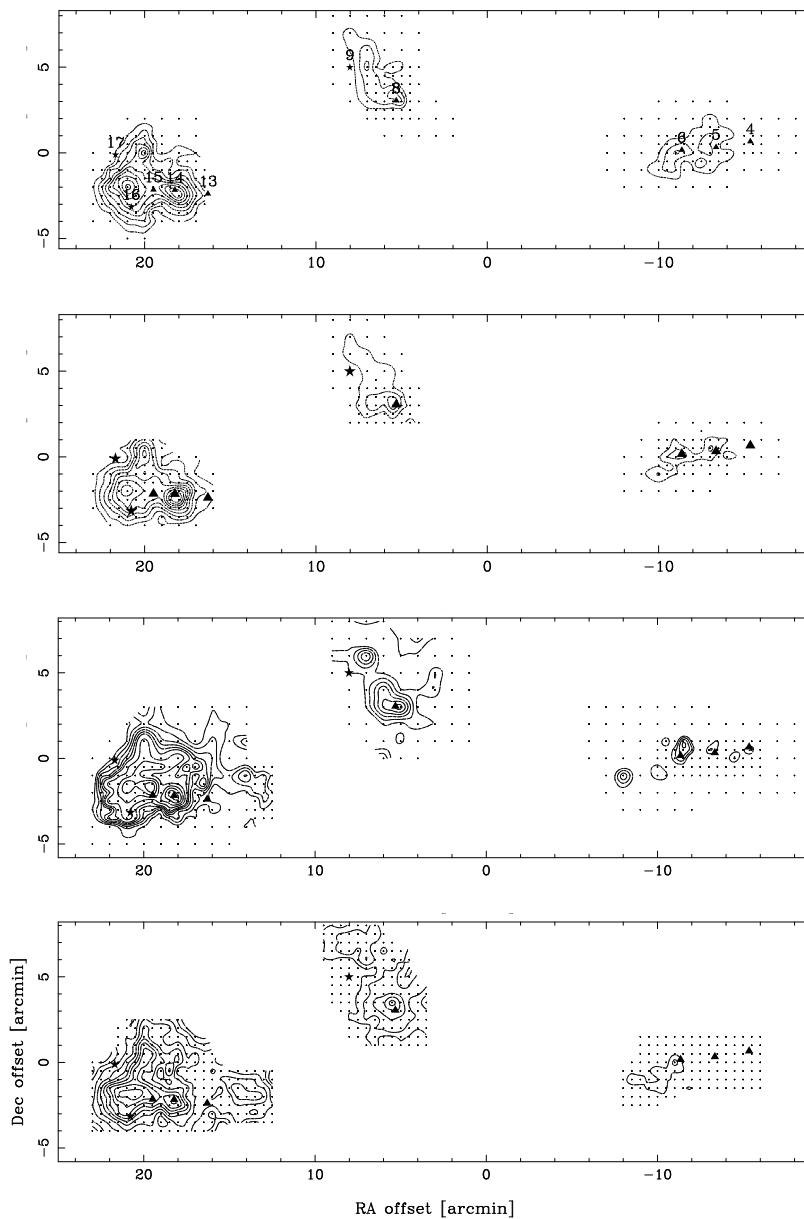


Figure 2: HNC, HCN, CS and HCO^+ (in descending order from top) integrated intensity maps of the $(-2, -6.5) \text{ km s}^{-1}$ velocity range (for HCN this range is the velocity range of the main, 2-1, component). The center position is $\alpha = 22^{\text{h}}33^{\text{m}} \delta = 74^{\circ}58'$ (1950.0) and the observed positions are indicated by dots. The intensity scale is in $T_A^* dv [\text{K km s}^{-1}]$. The HNC contours start at 0.9 and increase by 0.45 increments to 4.5 K km s^{-1} , for HCN contours range from 0.8 with 0.4 increment to 4.0 K km s^{-1} . For CS, contours are from 0.65 to 1.3 by 0.13 K km s^{-1} and from 1.3 to 2.34 by 0.26 K km s^{-1} , and for HCO^+ contours start from 0.8 and increase by 0.45 K km s^{-1} .

3. L 1251

L 1251 ($l \approx 114.52^\circ$, $b \approx +14.65^\circ$, $d = 300 \pm 50$ pc) is an active low-mass star forming region, with a number of young PMS stars and embedded YSOs detected (Kun & Prusti 1993, Kun 1998). Both position and cloud morphology suggest that this cloud has been/is being exposed to an external shock induced by 10^4 – 10^6 yr old supernovas, which might have triggered the star formation in the cloud. The cloud has three dense core groups, as revealed in the NH_3 survey of Tóth & Walmsley (1996). Using the 20-m telescope of the Onsala Space Observatory we mapped the ammonia "head" cores H1, H2 and H3, the northern core and the "tail" cores T1, T2 and T3, in the following dense gas molecular traces: CS, HNC, HCN and HCO^+ . In Table 2 we list the coordinates of the five selected positions which were observed in the rarer isotopomers ^{13}CO , C^{18}O , H^{15}NC , HN^{13}C , HC^{18}O^+ , and in the optically thin main isotopomer SO (the $3_3 - 2_1$ transition).

Table 2: Selected positions in the cloud observed in rare isotopomers. Offsets are relative to $\alpha = 22^h 33^m$, $\delta = 74^\circ 58'$.

	$\Delta\alpha$ [arcmin]	$\Delta\delta$ [arcmin]	YSO association
H 1a	21.0	-2.0	#16, T Tau, H_α
H 2a	19.5	-1.5	#15, ?
H 2b	18.0	-2.5	#14, IRAS 22376+7455
N 1	5.0	3.0	#8, IRAS 22343+7501
T 1a	-11.0	0	#6, embedded YSO

3. 1. MAPS

Figure 2 shows our maps. The stars denote the FIR point sources classified as T Tau stars, and the triangles those classified as embedded YSOs from Kun & Prusti (1993). Of the embedded YSOs, sources 8 and 14 are believed to power CO outflows (Sato et al. 1994). In all observed molecules the head part of the cloud has about 3–4 times stronger emission than the tail and the northern core. In CS total of 15 cores are detected, with radii ranging from 0.07 to 0.26 pc (standard deviation of the cores' radii is 0.02–0.07 pc for all available molecules). For the best defined cores the emission extents of all observed molecules agree, in most cases, within $\pm 1\sigma$ of the arithmetical mean. All but three cores have virial masses of about or less than $20 M_\odot$. An "excess" value of virial mass for H 1a, H 2b and N 1 cores may possibly be linked to the presence of T Tau stars, compact and extended outflows, respectively.

3. 2. MOLECULAR ABUNDANCES

In Table 3 we present the calculated LTE column densities of the observed rare isotopomers. From this data we derived fractional abundances of the main isomers, assuming local ISM relative abundances of atoms. For the CO species we used $T_{ex} = 10$ K, while for other molecules excitation temperatures of ~ 6 K were considered more appropriate. The H_2 column density was determined from C^{18}O using a conversion factor of $[\text{C}^{18}\text{O}]/[\text{H}_2] = 1.7 \times 10^{-7}$.

Table 3: LTE-derived total column densities. Units are in $[\text{cm}^{-2}]$. Ammonia data are from Tóth & Walmsley (1996).

Core	H 1a	H 2a	H 2b	N 1a	T 1a
^{13}CO [10 ¹⁵]	3.3	5.3	10.3	13.5	7.7
C^{18}O [10 ¹⁵]	0.9	1.8	2.8	2.6	1.0
C^{34}S [10 ¹²]	0.7	1.3	0.8	1.1	1.1
H^{13}CN [10 ¹¹]	6.5	4.4	5.1	1.7	7.5
HN^{13}C [10 ¹¹]	3.5	7.8	9.0	1.5	12.9
H^{15}NC [10 ¹¹]	1.4	1.9	1.3	1.7	2.7
SO [10 ¹²]	10.4	5.5	7.6	6.6	8.7
H^{13}CO^+ [10 ¹¹]	2.0	6.6	4.6	8.5	3.6
HC^{18}O^+ [10 ¹⁰]	8.5	–	7.8	–	–
NH_3 [10 ¹⁴]	17.8	–	9.9	–	22.2

3. 3. STAR FORMATION INFLUENCE ON CHEMISTRY

The presence of a T Tau star in H1 a would indicate an age of $10^6 - 10^7$ years for this core, while the embedded YSOs in the remaining 4 cores point to ages of $10^4 - 10^5$ years. The fractional abundances lack any clear trends with respect to the adopted dynamical ages of the cores. In an attempt to isolate trends suggested by chemical modelling, we have formed the abundance ratios of "late"-time (i.e., SO , HCO^+ , NH_3) relative to "early"-time molecules, that is CS , HCN and HNC (Table 3). If anything, the ratios point in general to trends opposite to the expected. We suggest that, if present chemical networks of dense and cold clouds predict the evolution of molecular abundances correctly, such trends are masked by the onset of processes like, e.g., star formation and external shocks.

References

- Berkhuijsen, E.M.: 1971, *Astron. Astrophys.* **14**, 252.
 Dickman, R.L. & Clemens, D.P.: 1983, *Astrophys. J.* **271**, 143.
 Grenier, I. A., et al.: 1989, *Astrophys. J.* **347**, 231.
 Johansson, L.E.B., Greve A., Booth R.S., et al.: 1998, *Astron. Astrophys.* **331**, 857.
 Kun, M. & Prusti, T.: 1993, *Astron. Astrophys.* **272**, 235.
 Kun, M., Vinkó, J., Szabados, L.: 2000, *Mon. Not. Roy. Astron. Soc.* **319**, 777.
 Kun, M.: 1998, *Astrophys. J. Suppl.*, **115**, 59.
 Sato, F. et al.: 1994, *Astrophys. J.* **435**, 279.
 Strong, A.W. & Mattox, J.R.: 1996, *Astron. Astrophys.* **308**, L21.
 Tóth, L.V. & Walmsley C.M.: 1996, *Astron. Astrophys.* **311**, 981.
 Yonekura, Y., Dobashi, K., Mizuno, A., et al.: 1997, *Astrophys. J. Suppl.*, **110**, 21.